Electronic Supplementary Material (ESI) for Journal of Materials Chemistry C.

Supplementary Information

Construction of Stable Luminescent Donor–Acceptor Neutral Radicals: A Theoretical Study

Xin Wang, Peiran Xue, Cefeng Zhou, Yewen Zhang, Ping Li*, Runfeng Chen*

State Key Laboratory of Organic Electronics and Information Displays & Jiangsu Key Laboratory for Biosensors, Institute of Advanced Materials (IAM), Nanjing University of Posts & Telecommunications, 9 Wenyuan Road, Nanjing 210023, China.

Contents

Computational details

All the calculations were carried out using the Gaussian 09 program. The geometries of the precursors and radicals were optimized using restricted and unrestricted density functional theory (DFT & UDFT)[1] with the Becker's three-parameter exchange functional along with the Lee Yang Parr's correlation functional (B3LYP) and 6-31G (d, p) basis set, respectively. The vibrational frequencies were analyzed at the same level to ensure that the optimized structures are at the real local minima with no imaginary frequency. All the geometries and relevant data were calculated in the gas phase. The spin density distributions and spin populations were obtained based on the optimized radical structures with isosurface value = 0.0004 (a.u.)[2]. The plane angle of radicals is derived from VMD software. For the calculations of ionization potential ($IP_{gas,298K}$) and electron affinity ($EA_{gas,298K}$), the molecular geometries and the sum of electronic and thermal energies are obtained at the B3LYP/6-31G(d) level. Nucleus independent chemical shift ($NICS_{iso}(1)$) was computed at 1 Å above the conjugated rings' plane with the gauge-independent atomic orbital (GIAO) method.[3] Anisotropy of the induced current density (AICD) plots were generated using the method developed by Herges et al[4] and ACID plots were generated with POV-Ray renderer. The fractional occupation number weighted electron density (N_{FOD}) is computed by the method developed by Grimme et al[5] using finite temperature density functional theory (FT-DFT) method with ORCA5.0.1 program package.[6] The buried volumes and steric maps presented in this work were obtained using the SambVca 2 Web application.[7]

Thermodynamic stability is related to the degree of generation of radical species and determines how many monomers are formed when the radical dimer is cleaved into a monomer.[8] The thermodynamic stability of radical species is evaluated by the indices such as bond dissociation energy (BDE)[9] and radical stabilization energy (RSE)[10]. BDE is the the reaction enthalpy required for homolytic cleavage of R-H into R• and H• shown in eqn (1), and thus depends exclusively on the relative enthalpies of formation of reactant and product states. RSE is expressed by the difference between the BDE (eqn (3)) of a radical species of interest and that of the radical selected as a reference (eqn (4)). In this work, the radical selected as the standard is TTM (eqn (2)). Either BDEs or RSEs can be used for evaluating the thermodynamic stability of radical species. However, RSE might be easier to evaluate the stability of radicals because RSEs indicate the relative stability to the TTM radicals.

$$\mathrm{R\text{-}H} \xrightarrow{\Delta H} \mathrm{R\bullet} + \mathrm{H\bullet} \quad (1)$$

$$\mathrm{TTM\bullet} + \mathrm{R\text{-}H} \xrightarrow{\Delta H} \mathrm{TTM\text{-}H} + \mathrm{R\bullet} \quad (2)\#\#$$

$$BDE(\mathrm{R\text{-}H}) = H(\mathrm{R\bullet}) + H(\mathrm{H\bullet}) - H(\mathrm{R\text{-}H}) \quad (3)\#$$

$$RSE(\mathrm{R\bullet}) = BDE(\mathrm{TTM\text{-}H}) - BDE(\mathrm{R\text{-}H}) \quad (4)\#$$

Here, $^{\mathrm{TTM\bullet}}$ stands for the $^{\mathrm{TTM}}$ radical, $^{\mathrm{R\bullet}}$ is the interested carbon-centered radicals, $^{\mathrm{TTM\text{-}H}}$ and $^{\mathrm{R\text{-}H}}$ represent the precursors of the corresponding radicals, and $^{\mathrm{H\bullet}}$ is the hydrogen radical. $H(^{\mathrm{R\bullet}})$ and $H(^{H\bullet})$ represent the reaction enthalpy of $^{\mathrm{R\bullet}}$ and $^{H\bullet}$, respectively.

Buried volume (V_{Bur}) is the total volume of a sphere with a defined radius (R) centered around a particular atom.[7] In this work, the center is the carbon radical with R = 6 Å, which gives a full view of the site resistance of the atoms surrounding the radical. The sphere volume ($^{V_{Sphere}}$) is the space around the carbon radical. This sphere is sectioned by a regular 3D cubic mesh of spacing, which defines cubic voxels $^{V_{xyz}}$ of volume. The

distance between the center of each voxel with all the atoms is tested to check if any of the atoms is within a van der Waals distance from the centre of the examined voxel. If no atom is within a van der Waals distance, the volume of the examined voxel is assigned to the free volume (V_{free}). Conversely, if a single atom is within a van der Waals distance, the volume of the examined voxel is assigned to V_{Bur}.

$$V_{Sphere} = \sum V_{xyz} = V_{free} + V_{Bur} = \sum V_{xyz}(\text{Free}) + \sum V_{xyz}(\text{Buried}) \#(5)$$

The percent of V_{Bur} can be described as $\%V_{Bur}$, and to present $\%V_{Bur}$ descriptor more intuitively, eqn (5) is simplified to eqn (6):

$$\%V_{Bur} = 100\% \times V_{Bur}/V_{Sphere} \#(6)$$

In the gas phase at 298 K and 1 atmosphere, $IP_{gas,298K}$ can be calculated by the enthalpy change the molecule M between the cationic (M^+) and neutral (M) molecules, while $EA_{gas,298K}$ by the difference between neutral (M) and anionic (M^-) molecules[11], as shown in eqn (7) and eqn (8):

$$IP_{gas,298K} = E_{M+} - E_M = \left(E_{Elec} + E_{ZPVE} + E_{them,298K}\right)_{M^+} - \left(E_{Elec} + E_{ZPVE} + E_{them,298K}\right)_M \#(7)$$

$$EA_{gas,298K} = E_M - E_{M-} = \left(E_{Elec} + E_{ZPVE} + E_{them,298K}\right)_M - \left(E_{Elec} + E_{ZPVE} + E_{them,298K}\right)_{M^-} \#(8)$$

where the enthalpy contains the total electronic energy (E_{Elec}), the zero-point vibrational energy (E_{ZPVE}) and thermal corrections ($E_{them,298K}$).

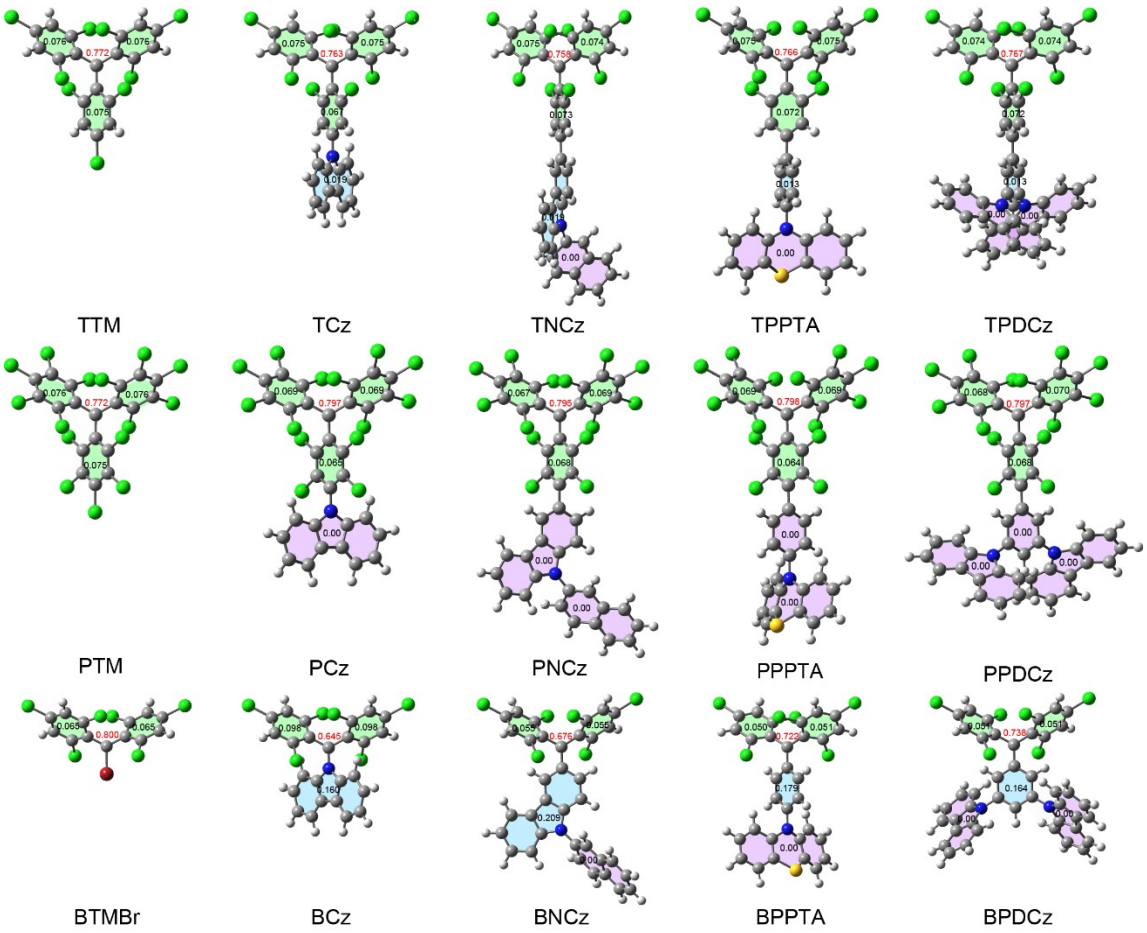

Figure S1. Spin populations of molecular fragments and the central carbon of the luminescent radicals (in red). The green fragment is the radical receptor, the blue and purple fragments are the donor, while the purple fragment refers to the spin populations of zero.

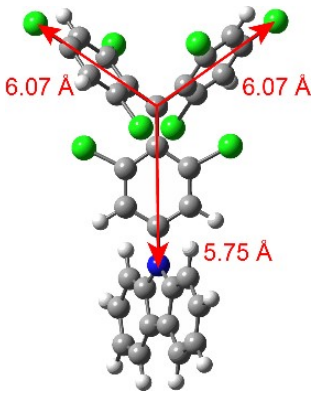

Figure S2. Optimized structure of TCz radical. The red arrow indicates the distance from the central carbon radical to other atoms.

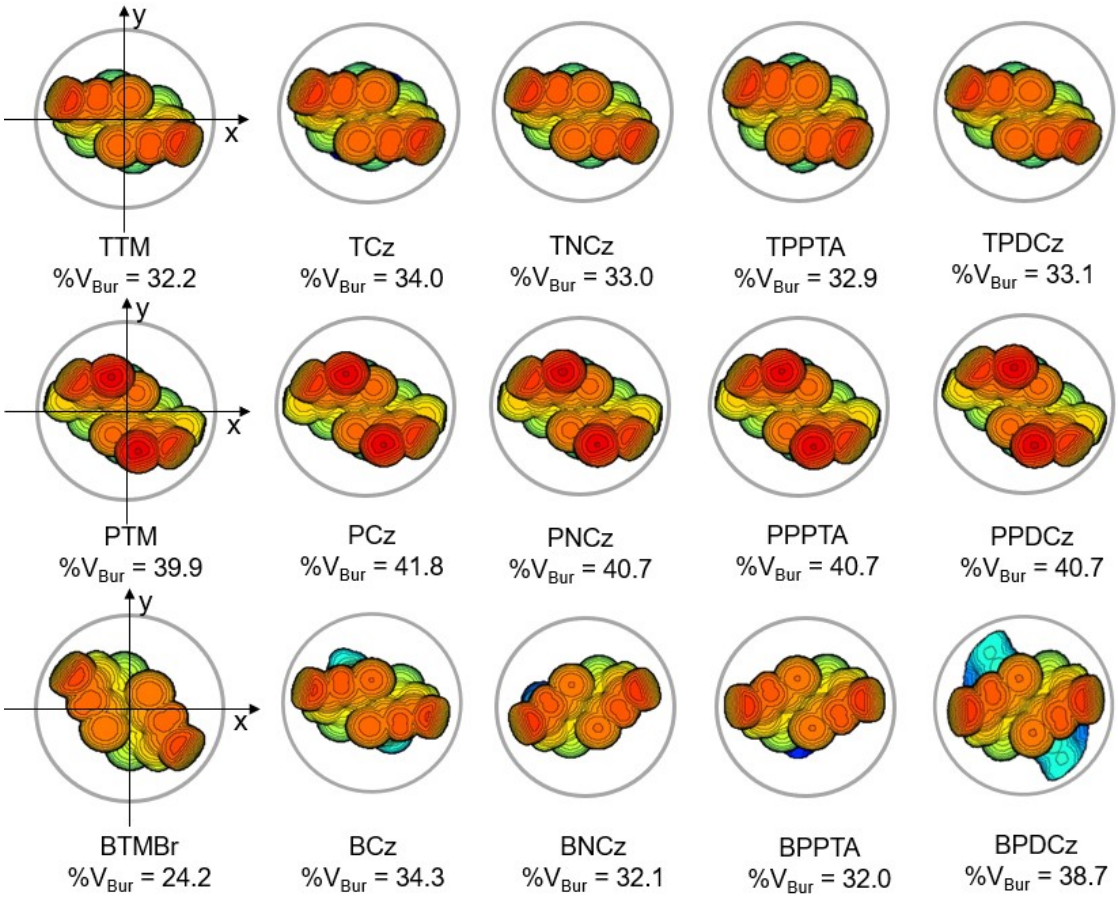

Figure S3. Steric maps and $\%V_{Bur}$ of radicals with the central carbon radical as the center of the sphere and 7 Å as the radius.

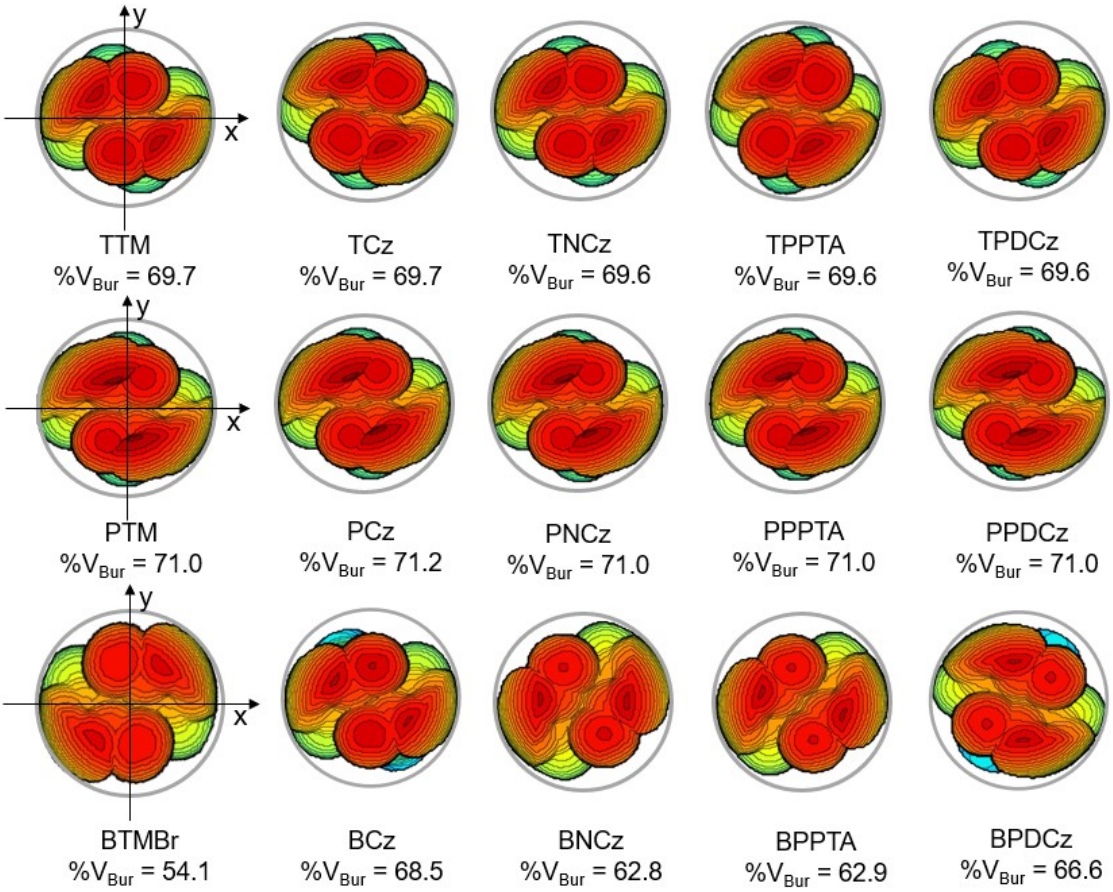

Figure S4. Steric maps and $\%V_{Bur}$ of radicals with the central carbon radical as the center of the sphere and 5 Å as the radius.

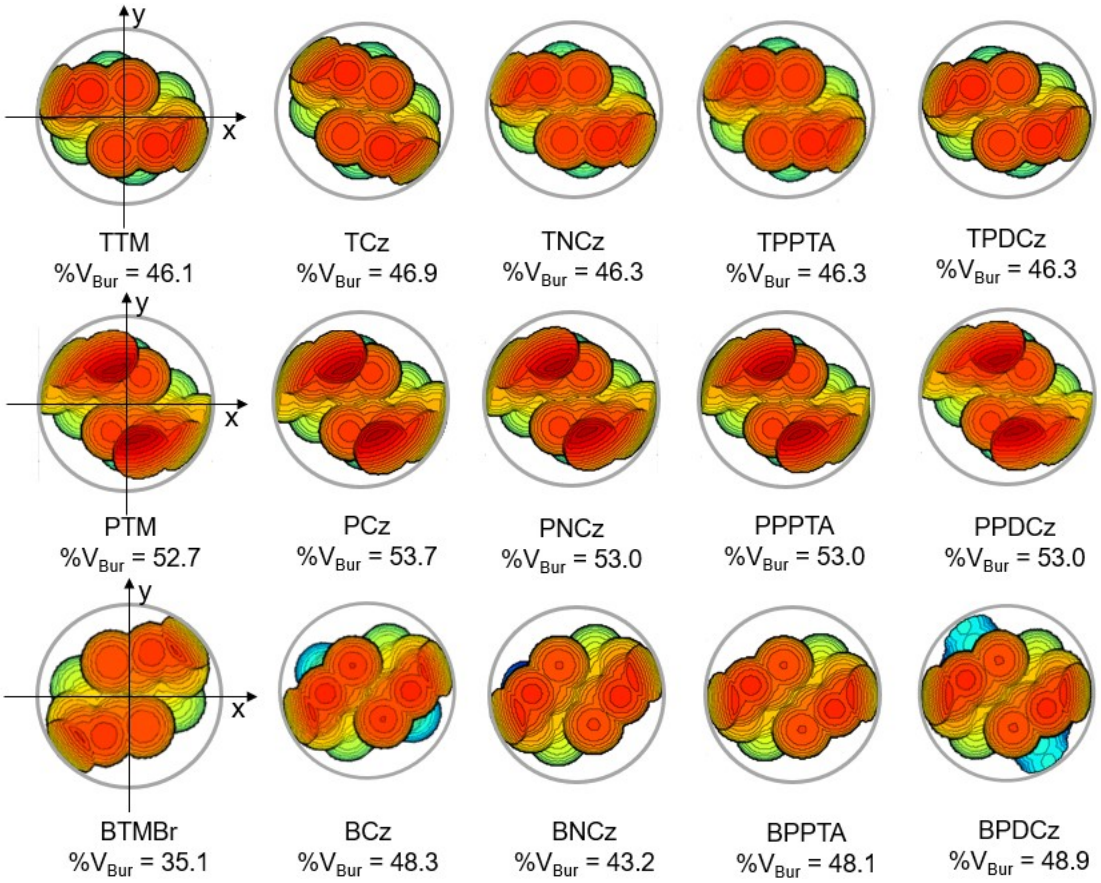

Figure S5. Steric maps and $\%V_{Bur}$ of radicals with the central carbon radical as the center of the sphere and 6 Å as the radius. Steric maps are viewed down the z axis. All these radii of 5~7 Å show consistent results, but the whole sphere appears to be a bit empty when the radius is 7 Å and the radius less than 6 Å cannot fully consider the spatial steric around the radical where the whole steric map is heavily occupied and hard to distinguish the protection of the surrounding atoms to the central carbon radical.

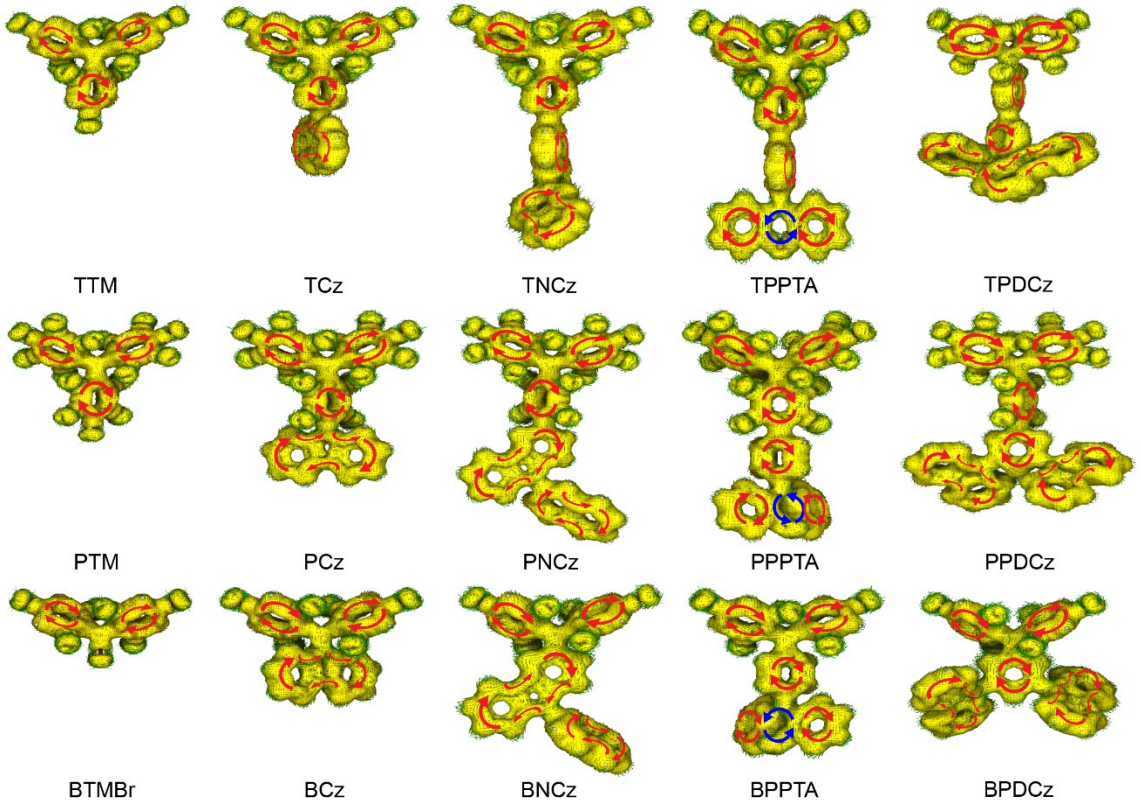

Figure S6. Anisotropy of the Induced Current Density (AICD) of molecules. The red and blue arrows indicate clockwise (diatropic: aromatic) and counterclockwise (paratropic: antiaromatic) ring current, respectively. The applied magnetic field is perpendicular to the molecular backbone and points out through the plane of the paper.

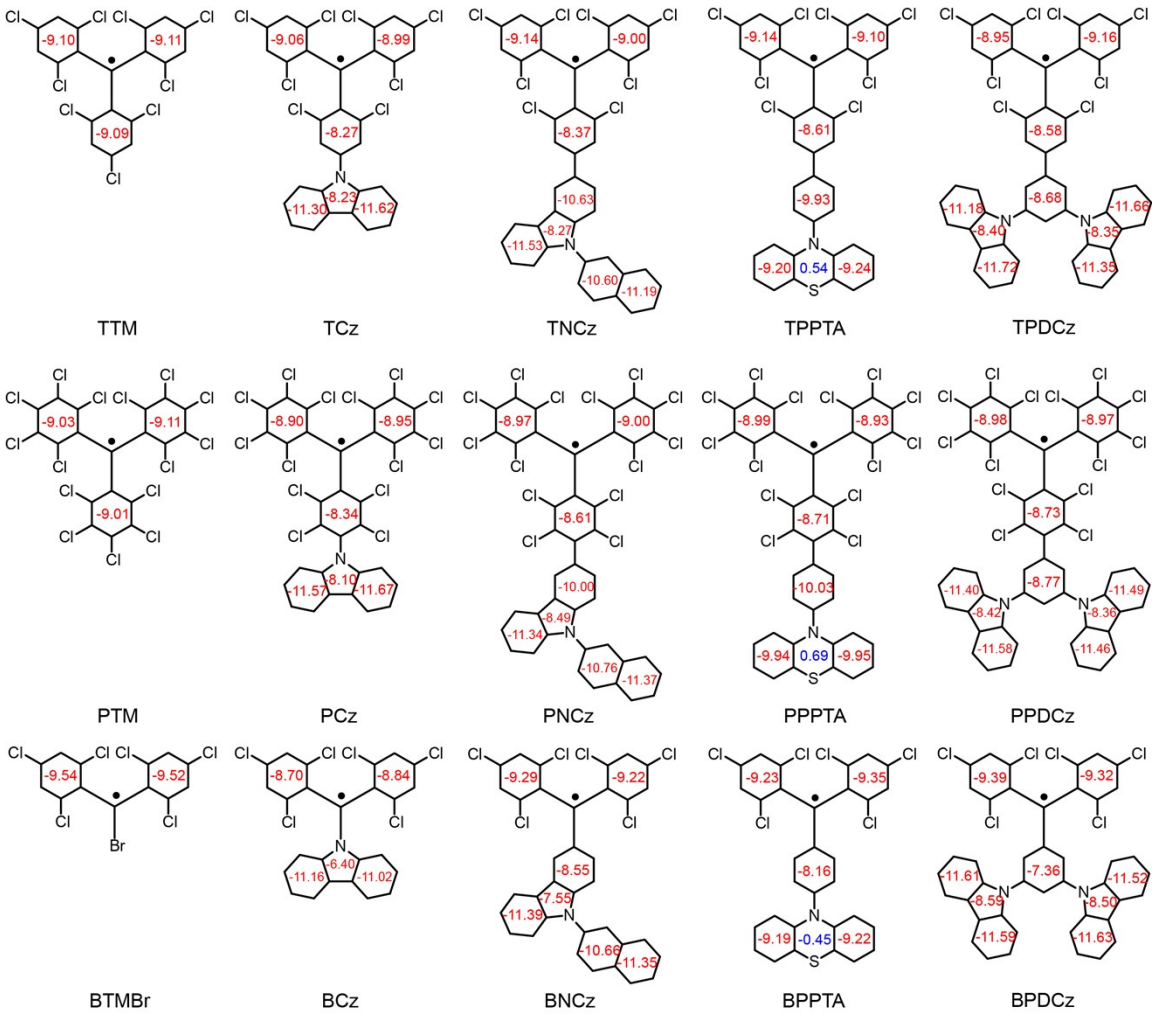

Figure S7. Nucleus independent chemical shift computed at 1 Å ($NICS_{iso}(1)$) above the ring's plane.

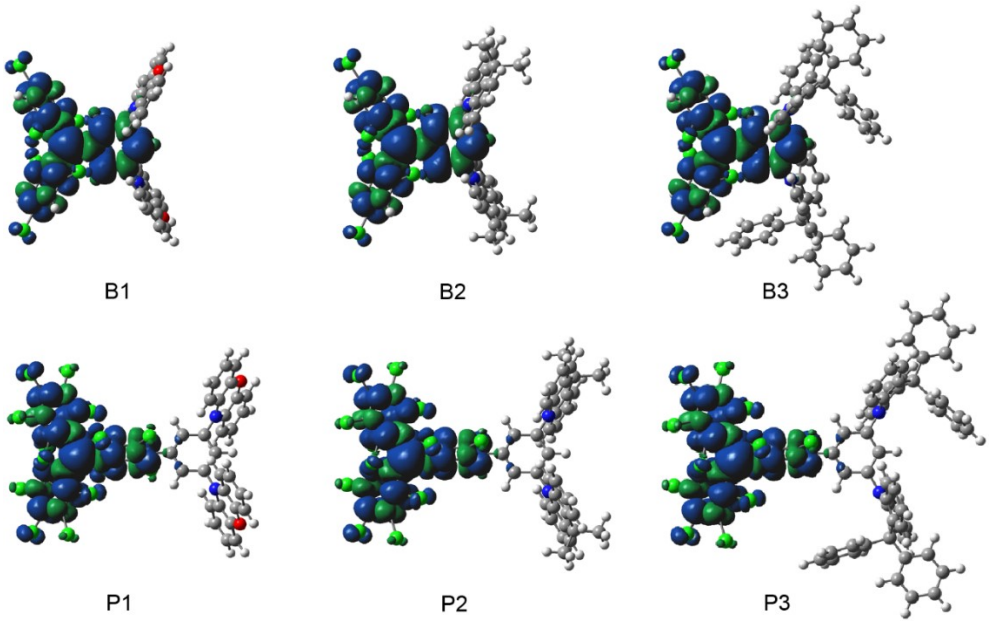

Figure S8. Spin density distributions of the designed high-perforemance BTM and PTM series radicals (isosurface value = 0.0004 a.u.).

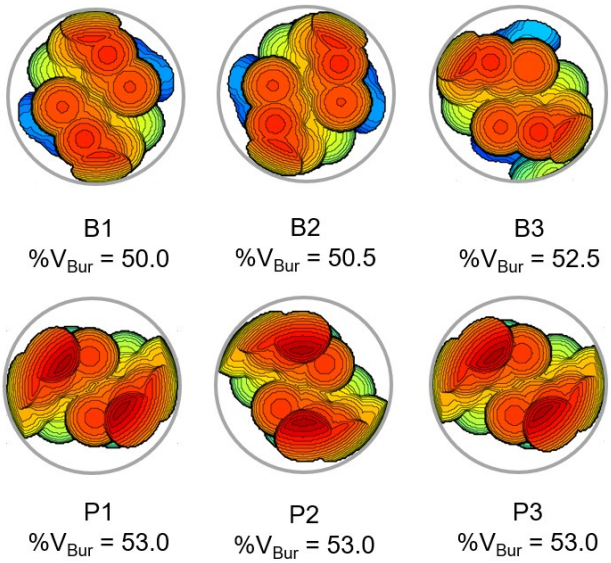

Figure S9. Steric maps and $\%V_{Bur}$ of the designed high-perforemance BTM and PTM series radicals. Steric maps are viewed down the z axis.

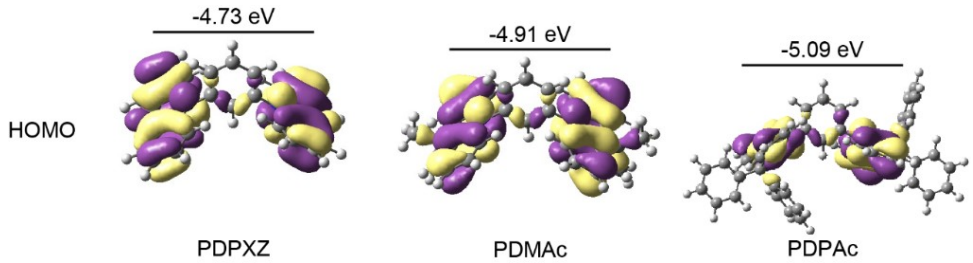

Figure S10. HOMO energy levels and electron distributions of the donor units.

Table S1. Enthalpies of radicals (*H*(R·)), hydrogen radical (*H*(H·)) and precursors of radicals (*H* (R-H)) as well as BDEs and RSEs of the luminescent stable radicals.

Molecule	*H*(R·)/ a.u.	*H*(H·)/ a.u.	*H*(R-H) / a.u.	BDE/ KJ mol^{-1}	RSE/ KJ mol^{-1}
TTM	-4869.14	-0.50	-4869.75	307.04	0.00
TCz	-4925.65	-0.50	-4926.27	306.21	0.82
TNCz	-5310.23	-0.50	-5310.85	305.83	1.21
TPPTA	-5554.79	-0.50	-5555.41	306.86	0.18
TPDCz	-5672.75	-0.50	-5673.36	306.91	0.12
PTM	-7626.67	-0.50	-7627.29	305.79	1.24
PCz	-7683.19	-0.50	-7683.81	305.97	1.07
PNCz	-8067.77	-0.50	-8068.38	305.82	1.22
PPPTA	-8312.33	-0.50	-8312.94	306.68	0.36
PPDCz	-8430.29	-0.50	-8430.9	306.25	0.79
BTMBr	-5830.47	-0.50	-5831.1	332.40	-25.36
BCz	-3775.48	-0.50	-3776.1	294.36	12.68
BNCz	-4160.06	-0.50	-4160.68	296.33	10.71
BPPTA	-4404.62	-0.50	-4405.24	301.64	5.4
BPDCz	-4522.58	-0.50	-4523.19	303.67	3.37

Table S2. Bond lengths of central carbon radical (R_1, R_2, and R_3) and that between radical acceptor and donors (R_4), as well as the angles between the two planes of the luminescent radicals.

Molecule	Bond Length (Å)				Planar Angle (°)[a]		
	R_1	R_2	R_3	R_4	∠αβ	∠αγ	∠βγ
TTM	1.474	1.474	1.475	1.749	49.0	-	-
TCz	1.475	1.475	1.472	1.410	48.4	82.4	49.8
TNCz	1.475	1.475	1.471	1.480	47.8	82.3	34.7
TPPTA	1.475	1.475	1.472	1.483	48.2	84.0	36.0
TPDCz	1.475	1.475	1.473	1.484	48.0	35.8	83.6
PTM	1.481	1.481	1.481	1.732	49.9	-	-
PCz	1.481	1.481	1.482	1.409	49.9	32.7	82.4
PNCz	1.482	1.481	1.481	1.493	49.7	26.8	76.2
PPPTA	1.481	1.481	1.482	1.495	50.3	28.4	78.4
PPDCz	1.481	1.481	1.481	1.496	49.4	42.7	88.6
BTMBr	1.465	1.465	-	1.395	-	-	-
BCz	1.467	1.467	-	1.393	-	43.9	-
BNCz	1.481	1.481	-	1.444	-	23.6	-
BPPTA	1.481	1.481	-	1.447	-	24.3	-
BPDCz	1.481	1.481	-	1.452	-	25.1	-

a: α refers to the central carbon radical plane, β is the plane of the radical fragment connected to the donor, and γ indicates the plane where the donor is located.

Table S3. Calculated ionization potential (IP) and electron affinity (EA) of radicals.

Molecule	E_M (a.u.)	E_{M+} (a.u.)	E_{M-} (a.u.)	IP (eV)	EA (eV)
TTM	-4869.14	-4868.88	-4869.21	7.09	-2.11
TCz	-4925.65	-4925.39	-4925.72	7.02	-1.80
TNCz	-5310.23	-5309.97	-5310.28	6.99	-1.35
TPPTA	-5554.79	-5554.57	-5554.85	5.96	-1.64
TPDCz	-5672.75	-5672.47	-5672.80	7.62	-1.38
PTM	-7626.67	-7626.41	-7626.78	7.27	-2.95
PCz	-7683.19	-7682.92	-7683.29	7.31	-2.68
PNCz	-8067.77	-8067.50	-8067.85	7.33	-2.20
PPPTA	-8312.33	-8312.06	-8312.42	7.22	-2.44
PPDCz	-8430.29	-8430.00	-8430.37	7.68	-2.17
BTMBr	-5830.47	-5830.21	-5830.54	7.19	-1.83
BCz	-3775.49	-3775.25	-3775.54	6.52	-1.59
BNCz	-4160.07	4159.83	-4160.10	6.52	-1.07
BPPTA	-4404.62	-4404.39	-4404.68	6.32	-1.52
BPDCz	-4522.58	-4522.30	-4522.63	7.56	-1.37

Table S4. Calculated radical stability index and stability improvement rate.

Molecule	RSE (KJ mol^{-1})	%V_{Bur}	IP (eV)	RSI (a.u.)	Stability improvement rate (a.u.)
TTM	0.00	46.1	7.09	1.55	0.00
TCz	0.82	46.9	7.02	1.94	0.25
TNCz	1.21	46.3	6.99	1.90	0.22
TPPTA	0.18	46.3	5.96	1.27	-0.18
TPDCz	0.12	46.3	7.62	2.24	0.44
PTM	1.24	52.7	7.27	2.01	0.00
PCz	1.07	53.7	7.31	2.48	0.27
PNCz	1.22	53.0	7.33	2.45	0.22
PPPTA	0.36	53.0	7.22	2.38	0.18
PPDCz	0.79	53.0	7.68	2.65	0.32
BTMBr	-25.36	35.1	7.19	0.72	0.00
BCz	12.68	48.3	6.52	2.03	1.84
BNCz	10.71	43.2	6.52	1.71	1.39
BPPTA	5.4	48.1	6.32	1.45	1.02
BPDCz	3.37	48.9	7.56	2.42	2.39

Table S5. Calculated RSE, %V_{Bur}, IP and radical stability index of designed high-perforemance BTM and PTM series radicals.

Molecule	RSE (KJ mol^{-1})	%V_{Bur}	IP (eV)	RSI (a.u.)
B1	4.17	50.0	7.24	2.58
B2	4.37	50.5	7.77	2.70
B3	4.40	52.5	8.18	2.79
P1	0.75	53.0	7.28	2.56
P2	0.80	53.0	7.82	2.67
P3	0.88	53.0	8.31	2.81

Reference:

1. W. Koch and M. Holthausen, *A Chemist Guide to Density Functional Theory*, 2001.
2. Y. Morita, S. Suzuki, K. Sato and T. Takui, *Nat. Chem.*, 2011, **3**, 197-204.
3. P. v. R. Schleyer, M. Manoharan, Z. Wang, B. Kiran, H. Jiao, R. Puchta and N. J. R. van Eikema Hommes, *Org. Lett.*, 2001, **3**, 2465-2468.
4. R. Herges and D. Geuenich, *J. Phys. Chem. A*, 2001, **105**, 3214-3220.
5. S. Grimme and A. Hansen, *Angew. Chem. Int. Ed.*, 2015, **54**, 12308-12313.
6. F. Neese, *WIREs Computational Molecular Science*, 2012, **2**, 73-78.
7. L. Falivene, Z. Cao, A. Petta, L. Serra, A. Poater, R. Oliva, V. Scarano and L. Cavallo, *Nat. Chem.*, 2019, **11**, 872-879.
8. T. Kubo, *Molecules*, 2019, **24**, 665.
9. S. J. Blanksby and G. B. Ellison, *Acc. Chem. Res.*, 2003, **36**, 255-263.
10. P. Li, S. Wang, Z. Wang, C. Zheng, Y. Tang, Q. Yang, R. Chen and W. Huang, *J. Mater. Chem. C*, 2020, **8**, 12224-12230.
11. D. Wang, S. Huang, C. Wang, Y. Yue and Q. Zhang, *Org. Electron.*, 2019, **64**, 216-222.